Available online at www.sciencedirect.com

SCIENCE DIRECT®

Journal of Sound and Vibration 281 (2005) 1133–1144

JOURNAL OF SOUND AND VIBRATION

www.elsevier.com/locate/jsvi

Analytical study of multi-particle damping

M. Saeki*

[a] Department of Mechanical and Control Engineering, Niigata Institute of Technology, Fujihashi, Kashiwazaki, Niigata 945-1195, Japan

Received 22 April 2003; received in revised form 16 December 2003; accepted 12 February 2004

Abstract

Multi-unit particle dampers are passive damping devices involving granular particles in some cavities of a primary system. The principle behind particle damping is the removal of vibratory energy through losses that occur during impact of granular particles. This paper presents the results of experimental and analytical studies of the performance of a multi-unit particle damper in a horizontally vibrating system. An analytical solution based on the discrete element method is presented. Comparison between the experimental and analytical results shows that accurate estimates of the rms response of a primary system can be obtained. It is shown that the response of the primary system depends on the number of cavities and cavity dimensions.

1. Introduction

Particle dampers, also known as shot dampers [1] or granular-fill dampers [2], are passive damping devices. The principle behind particle damping is the removal of vibratory energy through losses that occur during impact of granular particles which move freely within the boundaries of a cavity attached to a primary system. Particle damping with suitable materials can be performed in a wider temperature range than most other forms of passive damping. Therefore, it can be applied in extreme temperature environments, where most conventional dampers would fail. The damping efficiency of particle damping depends on cavity dimensions. When the

*Tel.: +81-257-22-1195; fax: +81-257-22-1195.
E-mail address: saeki@mce.niit.ac.jp (M. Saeki).

0022-460X/$ - see front matter
doi:10.1016/j.jsv.2004.02.034

optimum dimensions of the cavity are large, the optimum cavity may not be attached from a practical design point of view. In such a case, the damper performance is retained when particle dampers are replaced by multi-unit dampers with a moderate number of small cavities.

Many experimental and analytical studies have demonstrated the effectiveness of particle dampers [1–14]. Although these studies described the damping effects in detail, most analytical results have focused on multi-particle single-unit dampers or single-particle multi-unit dampers. In order to develop a comprehensive design methodology for multi-particle multi-unit dampers (it is termed 'multi-unit particle dampers' as follows), an effective numerical method is required.

The objective of this work is to construct an analytical model for calculating the performance of multi-unit particle damping using some cylindrical cavities. The model is based on the discrete element method (also known as 'DEM', [15]). First, the validity of the analytical model of a multi-unit particle damper in a horizontally vibrating system is examined by comparison with experimental results. Subsequently, the relationship between the behavior of the granular particles in the cavities and the damper performance is presented. Finally, the influence of the number of cavities and the cavity dimensions on the damping performance is investigated.

2. Multi-unit particle damper

Fig. 1 shows a model of a multi-unit particle damping system. The x–z plane is parallel to the horizontal plane. The primary system is constrained to move only in the x-direction. The harmonic motion of the support point U (amplitude a and angular frequency ω) excites the primary system with linear spring k, mass M and viscous damping c. The primary system has some cylindrical cavities, which are attached symmetrically with respect to the x-axis. Although the cavities are not limited in number, the maximum usable number of cavities is 5 in this paper. When the same amount of granular particles is placed in each cavity of the primary system, as shown in Fig. 1, each collision of the particles with the wall of the cavities results in an exchange of momentum and some energy dissipation, attenuating the primary system's motion.

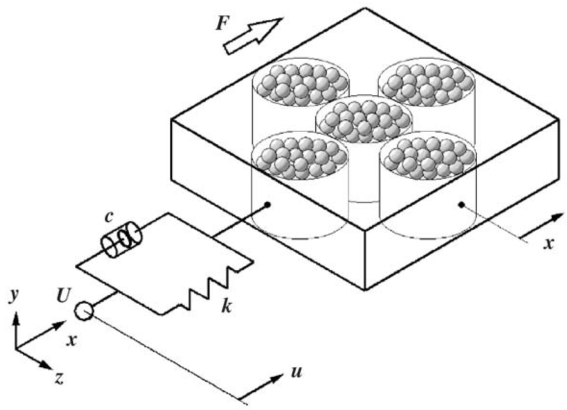

Fig. 1. Model of a multi-unit particle damping system.

The effectiveness of the multi-unit particle damper depends particle size and particle number. Therefore, the motion of all particles should be considered in order to analyze the motion of the primary system in detail. The equation of motion for particle i is given by

$$
\begin{aligned}
m\ddot{\mathbf{p}}_i &= \mathbf{F} - m\mathbf{g}, \\
I\boldsymbol{\varphi}_i &= \mathbf{T}_i,
\end{aligned}
\tag{1}
$$

where m is the particle mass, I is the moment of inertia of the particle and $\mathbf{g}$ is the acceleration vector due to gravity. $\mathbf{p}$ is the position vector of the center of gravity of the particle, $\boldsymbol{\varphi}$ is the angular velocity vector, and $\mathbf{F}$ is the sum of the contact forces acting on the particle. $\mathbf{T}$ is the sum of the torque caused by the contact forces. The dots denote time derivatives. In this study, an assembly of spherical particles of the same size is used.

The equation of motion for the primary system is expressed as

$$
\begin{aligned}
&M\ddot{x} + c(\dot{x} - \dot{u}) + k(x - u) = F, \\
&u = a \cos \omega t,
\end{aligned}
\tag{2}
$$

where F is the component of the contact force of the primary system with the particles in the direction of excitation and u is the harmonic displacement of the support point. a is the amplitude and ω is the angular frequency.

Although the effect of the behavior of granular particles on the damping efficiency can be analyzed using Eqs. (1) and (2), it requires considerable computational effort: consequently, the following approach is used to estimate the effectiveness of the damper. On the assumption that the behaviors of the granular particles in each cavity are the same, the contact force of the primary system with all particles can be considered to be equal to the product of the number of cavities and the contact force of the primary system with the particles in a cavity. Therefore, the particle number that should be considered in the numerical simulation can be reduced to the particle number in a cavity. This convenience makes it possible to considerably reduce the calculation time.

According to the above assumption, the equation of motion for the primary system can be expressed in the following form instead of Eq. (2):

$$
M\ddot{x} + c(\dot{x} - \dot{u}) + k(x - u) = N_U \times F_u,
\tag{3}
$$

where F_u is the component of the contact force of the primary system with the particles in a cavity along the direction of excitation and N_U is the number of cavities.

3. Contact force

Consider the contact problem between two particles i and j. The contact force acting on particle i can be divided into normal and tangential components. The normal component $\mathbf{f}_n$ of the contact force is modeled by the sum of the spring force based on Hertzian contact theory and the damping force [16] and expressed as in the following Eq. (4). The tangential component $\mathbf{f}_t$ of the contact force is given in Eq. (5), considering Coulomb's law of friction.

$$\mathbf{f}_n = k_n \delta_n^{3/2} + c_n \delta_n^{1/4} \dot{\delta}_n, \tag{4}$$

$$\mathbf{f}_t = -\mu f_n \dot{\delta}_t / \left| \dot{\delta}_t \right|, \tag{5}$$

where δ_n and $\dot{\delta}_n$ are the normal displacement and velocity of particle i relative to particle j, respectively. δ_t is the tangential velocity, and c_n and μ are the damping constant and the coefficient of friction between two particles or between a particle and the cavity wall, respectively.

For inter-particle behavior and particle/wall interaction, normal displacement δ_n is given by

$$\delta_n = 2r - \left| \mathbf{p}_j - \mathbf{p}_i \right|, \tag{6}$$

$$\delta_n = r - s, \tag{7}$$

respectively, where r and s are the particle radius and the distance between the center of the particle and the cavity wall, respectively. $\mathbf{p}$ is the position vector of the center of gravity of the particle.

For particle contact with a cylindrical wall, normal displacement δ_n is given by

$$\delta_n = \sqrt{(x_i - x_M)^2 + (y_i - y_M)^2} + r - R, \tag{8}$$

where R and subscript M are the radius and the center of the cylindrical cavity, respectively. x_i and y_i are the coordinates of particle i. Therefore, both an inter-particle contact and a particle/wall contact are realized if $\delta_n > 0$.

In Eq. (4), k_n is the spring constant and is defined according to the Hertzian contact theory [17]. In the case of the inter-particle contact [17], k_n is expressed as

$$k_n = \frac{\sqrt{2r}}{3} \frac{E_p}{1 - v_p^2}, \tag{9}$$

where E and v are the modulus of the elasticity and the Poisson ratio, respectively. Subscript p denotes the particle.

In the case of contact between a sphere and the flat wall [17], k_n is expressed as

$$k_n = \frac{4\sqrt{r}}{3} \frac{E_p E_0}{(1 - v_p^2) E_0 + (1 - v_0^2) E_p}, \tag{10}$$

where subscript 0 denotes the wall.

In the case of contact between a sphere and the cylindrical wall of the cavity [17], k_n is expressed as

$$k_N = \sqrt{\frac{128}{9} \zeta} \frac{E_i E_0}{(1 - v_i^2) E_0 + (1 - v_0^2) E_i}, \tag{11}$$

where ζ is a constant that is dependent on the cavity radius R and particle radius r. When the particle radius r is constant, the relationship between the cavity radius R and ζ is shown in Fig. 2 [17]. By using the relationship, the effect of the cavity radius R on the spring constant k_n is shown in Fig. 3. This figure also shows the spring constant k_n in the case of contact between a sphere and

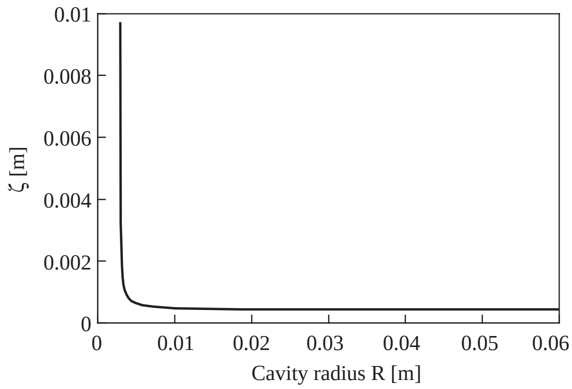

Fig. 2. Relation between the cavity radius R and ζ ($r = 0.003$ m).

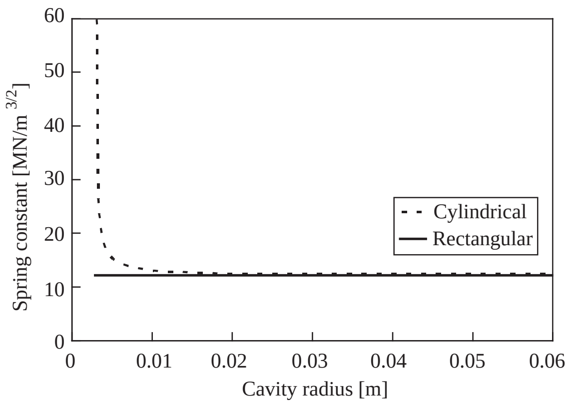

Fig. 3. Influence of the cavity radius on the spring constant ($r = 0.003$ m).

the flat wall. It can be seen that both are almost the same for the cavity radius $R > 0.02$ m. Thus, in the case of particle contact with the cylindrical wall, the spring constant k_n can be given by Eq. (10) for $R > 0.02$ m.

For the damping force in Eq. (4), the damping constant c_n is a function of the coefficient e of restitution [16]. Therefore, the value of c_n can be determined by the coefficient e of restitution.

Each particle may be in contact with many other particles and the wall simultaneously. Therefore, the sum $\mathbf{F}$ of the contact force acting on the particle and the sum $\mathbf{T}$ of the torque caused by the contact force are given by

$$\mathbf{F}_i = \sum (\mathbf{f}_n + \mathbf{f}_t), \tag{12}$$

$$\mathbf{T}_i = \sum (r_i \mathbf{n}_{ij} \times \mathbf{f}_t), \tag{13}$$

where $\mathbf{n}_{ij}$ is the unit vector from the center of particle i to the center of particle j.

Here, the procedure for calculation is described. First, consider the motion of a particle and determine the contact force acting on the particle, using Eqs. (4)–(10). Then the same procedure is repeated for particles in a cavity. In addition, the component of the contact force acting on the primary system along the direction of excitation is given by the summation of the contact forces between the particles and the wall of a granular-particle-filled cylinder. The behavior of the entire system is determined by the integration of the equations of motion for the primary system (Eq. (3)) and particles (Eq. (1)) over time.

4. Experimental verification

Fig. 4 shows the experimental apparatus used in this study. The experimental apparatus consists of the primary structure, and acts as an equivalent single-degree-of-freedom system. The structure is supported by four leaf springs and the equivalent properties are $M = 1.319\,\mathrm{kg}$, $c = 0.877\,\mathrm{N\,s/m}$ and $k = 3493.2\,\mathrm{N/m}$. The particle damper consists of five cylindrical cavities, which are made of acrylic resin. In Fig. 4, the dimensions of the cavity are $R = 0.03\,\mathrm{m}$ and $H = 0.03\,\mathrm{m}$, where H denotes the maximum height that the particles can reach. The primary system is excited sinusoidally at the support by means of a horizontally vibrating shaker. The motion of the primary system was measured with an accelerometer. The impacting granular spherical particles in each cavity used in this study are made of acrylic resin, and are of uniform size ($r = 0.003\,\mathrm{m}$). To investigate the effect of the number of cavities on the damping efficiency, 3, 4 and 5 cavities were partially filled with granular particles of the same number, as shown in Fig. 5.

Fig. 6 shows the comparison between the analytical predictions and measured time history of the primary system's motion. This figure shows the steady-state vibration after the transient response has been allowed to decay. There is little difference between the analytical values and the experimental values for the time history.

Figs. 7–9 show comparison of the experimental results with the calculated ones. All the figures show plots of the root mean square (rms) value of the primary system amplitude versus the frequency ($f = \omega/2\pi$). In these figures, λ is the mass ratio, which is the total mass of granular

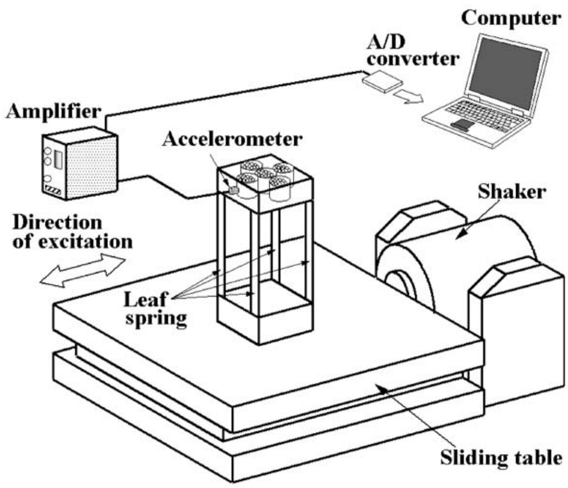

Fig. 4. Schematic of experimental apparatus.

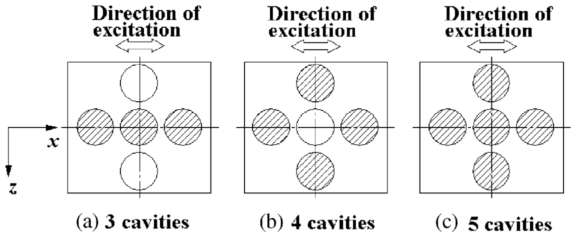

Fig. 5. Cavity arrangement.

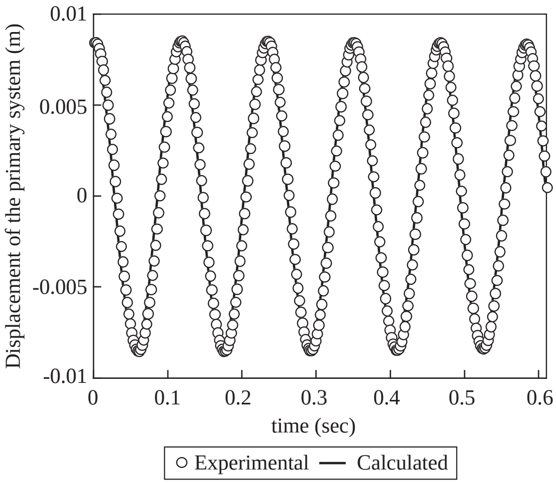

Fig. 6. Comparison between experimental and calculated results ($a = 0.001$ m, $f = 8.3$ Hz, 5 cavities, $\lambda = 0.098$).

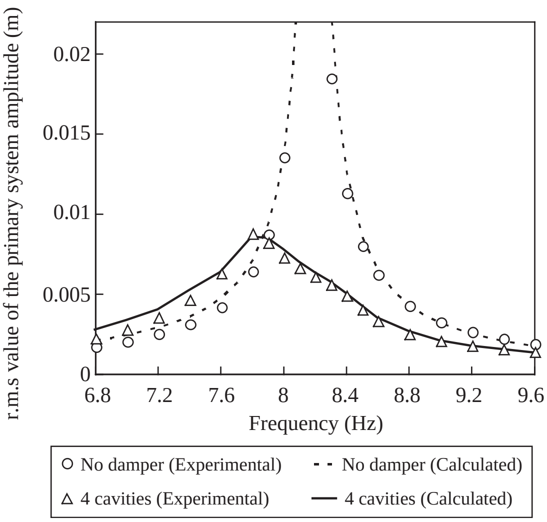

Fig. 7. Comparison between experimental and calculated results ($a = 0.001$ m, 4 cavities, $\lambda = 0.098$).

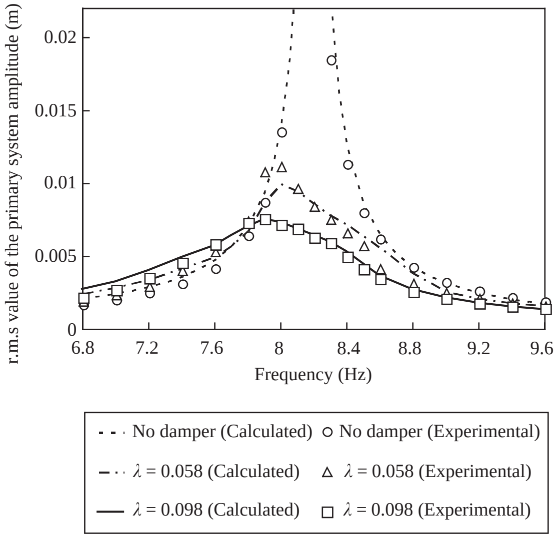

Fig. 8. Comparison between experimental and calculated results ($a = 0.001$ m, 5 cavities).

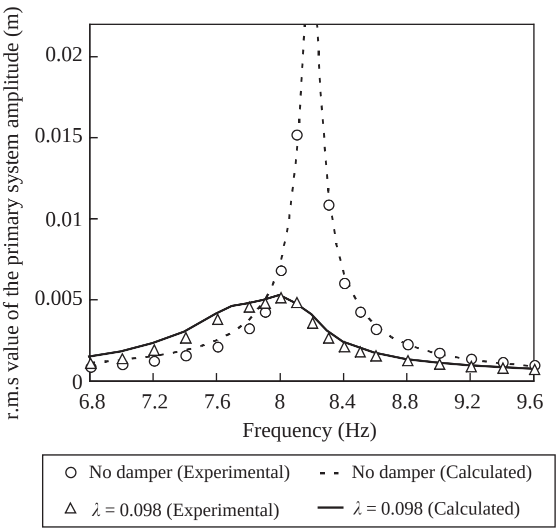

Fig. 9. Comparison between experimental and calculated results ($a = 0.0005$ m, 5 cavities, $\lambda = 0.098$).

particles divided by the mass of the primary system. The computational conditions used for the simulation are shown in Table 1. In Figs. 7 and 8, the numbers of cavities used are 4 and 5, respectively. The amplitude is smaller for Fig. 9 than that for Figs. 7 and 8. Clearly, for the range of system parameters used in the experimental phase of this study, the calculated results reproduce the experimental results with reasonable accuracy. Therefore, the approach in this study is effective for estimating the damping effect of multi-unit particle dampers.

Table 1
Values of parameters in granular materials

Total number	564~957
Diameter (m)	0.006
Density (kg/m^3)	1190
Coefficient of friction μ	0.52
Damping constant α	0.077
Spring constant (N/m$^{3/2}$)	
Particle–particle	1.0×10^7
Particle–wall	1.3×10^7

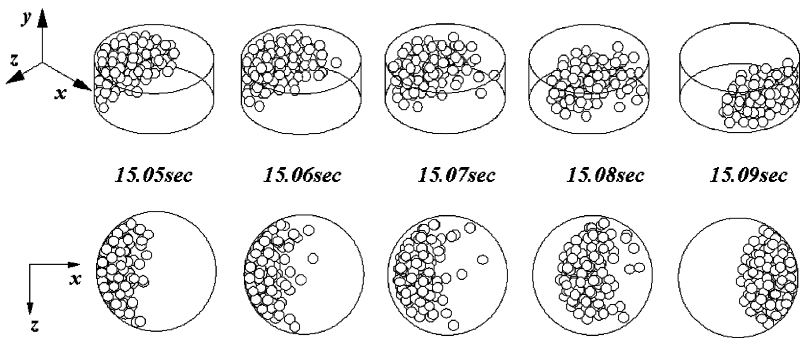

Fig. 10. Behavior of granular materials in a cavity ($a = 0.001$ mm, 5 cavities, $\lambda = 0.058$, $R = 0.03$ m).

5. Analytical results

In this section, the effectiveness of the multi-unit particle damper is discussed in terms of the analytical results. The multi-unit particle damping system is excited by a harmonic motion of its support, $u = a \sin \omega t$, as shown in Fig. 1. The computational conditions were carried out under identical conditions as mentioned in Section 4. Figs. 10 and 11 show examples of the behavior of granular particles in a cavity obtained by the numerical simulation. In the case of Figs. 10 and 11, mass ratios λ are 0.058 and 0.098, respectively. It is observed that, as time passes, granular particles move in the direction of excitation. For $\lambda = 0.058$, the motion of the upper layer of granular particles is very active, as shown in Fig. 10. In the case of Fig. 11, granular particles move as a lump. The number of particles, which make contact with the floor of the cavity, is larger for Fig. 11 than for Fig. 10. Thus, the effect of the friction between particles and the cavity wall on the damping efficiency seems to increase as the mass ratio increases.

Figs. 12 and 13 show plots of the response of the primary system versus the frequency. The cavity radius is larger for Fig. 13 than for Fig. 12. In Fig. 12, the resonance amplitude of the primary system decreases as the mass ratio λ decreases. It is also found that the maximum amplitude occurs at a lower frequency for $\lambda = 0.098$ than for $\lambda = 0.058$. However, this trend is different from that in Fig. 13. In the case of Fig. 13, the maximum amplitude occurs at almost the same frequency and the maximum amplitude is smaller for $\lambda = 0.098$ than for $\lambda = 0.058$. The reason for the difference seems to be that it is more difficult for granular particles to move as the cavity radius decreases.

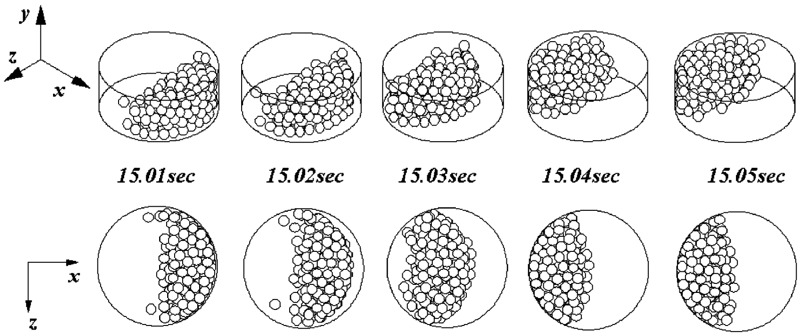

Fig. 11. Behavior of granular materials in a cavity ($a = 0.001$ m, 5 cavities, $\lambda = 0.098$, $R = 0.03$ m).

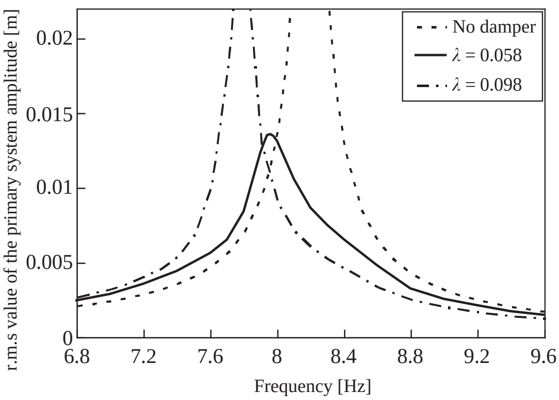

Fig. 12. Response of the primary system amplitude versus the frequency ($a = 0.001$ m, 3 cavities, $R = 0.03$ m).

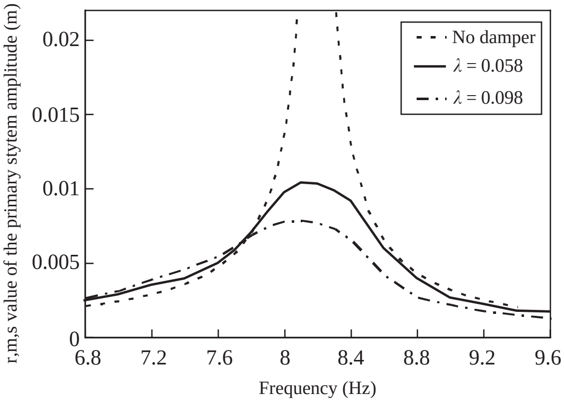

Fig. 13. Response of the primary system amplitude versus the frequency ($a = 0.001$ m, 3 cavities, $R = 0.038$ m).

Fig. 14 shows the relationship between the maximum r.m.s. value of the primary system amplitude and the cavity radius R. This figure also shows the effect of the mass ratio on the damping performance. In the case of 5 cavities, the maximum rms value of the primary system

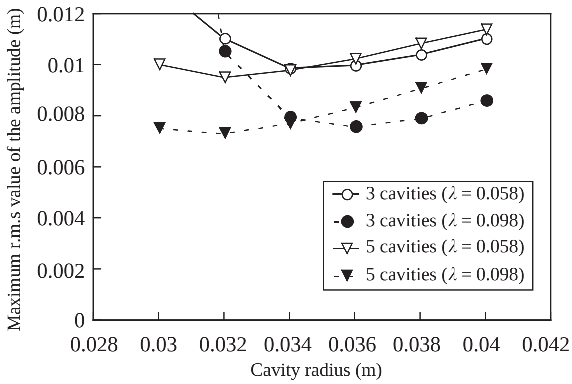

Fig. 14. Influence of the cavity radius on the damping efficiency ($a = 0.001$ m, $f = 8.3$ Hz).

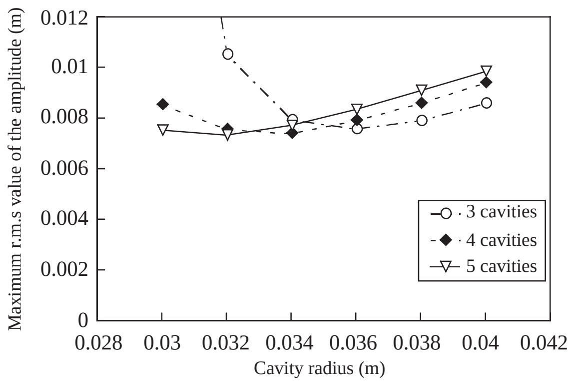

Fig. 15. Influence of the cavity number on the damping efficiency ($a = 0.001$ m, $f = 8.3$ Hz, $\lambda = 0.098$).

amplitude is always larger for $\lambda = 0.058$ than for $\lambda = 0.098$. This trend is different from that for 3 cavities. For the cavity radius $R < 0.032$ m, the maximum rms value of the primary system amplitude is smaller for $\lambda = 0.058$ than for $\lambda = 0.098$.

Fig. 15 shows the effect of the unit number on the optimum cavity radius R. The effect of the cavity radius on the maximum rms value of the primary system amplitude is more significant as the unit number decreases. For all the cases of cavities used, it is clear that maximum rms values of the primary system amplitude at the optimum cavity radius are almost the same. In addition, the optimum cavity radius R decreases with increasing unit number. The reason is that the mobility of granular particles in a cavity increases as the unit number increases.

6. Conclusions

This paper has presented an analytical model to simulate the damping performance of a multi-unit particle damper in a horizontally vibrating system. Comparison between the theory and the experiment was found to be remarkably good. It is shown that the damping performance chiefly depends on the relationship between the mass ratio and the number of cavities. It is also shown that the optimum cavity radius decreases with increasing unit number. Also, for the range of system parameters used in this study, it is clear that maximum rms values of the primary system amplitude at the optimum cavity radius are almost the same.

References

[1] C. Cempel, G. Lotz, Efficiency of vibration energy dissipation by moving shot, *Journal of Structural Engineering* 119 (9) (1993) 2642–2652.
[2] L. Salvino, P. Dupont, J.G. McDaniel, Evaluation of granular-fill damping in shock loaded box beams, *Proceedings of the 69th Shock and Vibration Symposium*, 1998, pp. 1–10.
[3] S.F. Masri, Motion and stability of two-particle single-container impact dampers, *Journal of Applied Mechanics* 34 (1967) 506–507.
[4] S.F. Masri, Effectiveness of two-particle impact damper, *Journal of the Acoustical Society of America* 41 (1967) 1533–1554.
[5] S.F. Masri, Analytical and experimental studies of multiple-unit impact dampers, *Journal of the Acoustical Society of America* 45 (5) (1969) 1111–1117.
[6] S.F. Masri, Periodic excitation of multiple-unit impact dampers, *ASCE Journal of the Engineering Mechanics Division* 96 (5) (1970) 1195–1207.
[7] Y. Araki, I. Yokomichi, J. Inoue, Impact dampers with granular materials, *JSME* 28 (241) (1985) 1466–1472.
[8] H.V. Panossian, Structural damping enhancement via non-obstructive particle damping technique, *Journal of Vibration and Acoustics* 114 (1992) 101–105.
[9] T. Sato, K. Tanaka, S. Aida, Y. Mouri, Vibration isolation in a system using granular medium, *JSME International Journal Series C* 38 (3) (1995) 434–440.
[10] I. Yokomichi, Y. Araki, Y. Jinnouchi, J. Inoue, Impact damper with granular materials for multibody system, *Journal of Pressure Vessel Technology* 118 (1996) 95–103.
[11] A. Papalou, S.F. Masri, Performance of particle dampers under random excitation, *Journal of Vibration and Acoustics* 118 (1996) 614–621.
[12] R.D. Friend, V.K. Kinra, Particle impact damping, *Journal of Sound and Vibration* 233 (1) (2000) 93–118.
[13] G.R. Tomlinson, D. Pritchard, R. Wareing, Damping characteristics of particle dampers—some preliminary results, *Proceedings of the Institute of Mechanical Engineers* 215 (2001) 253–257.
[14] M. Saeki, Impact damping with granular materials in a horizontally vibrating system, *Journal of Sound and Vibration* 251 (1) (2002) 153–161.
[15] P.A. Cundall, O.D. Struck, A discrete numerical model for granular assemblies, *Geotechnique* 29 (1979) 47–65.
[16] Y. Tsuji, T. Tanaka, T. Ishida, Lagrangian numerical simulation of plug flow of cohesionless particles in a horizontal pipe, *Powder Technology* 71 (1992) 239–250.
[17] Japan Society of Mechanical Engineers, *JSME Mechanical Engineer's Handbook*, Maruzen, Tokyo, 1990.